The Journal of Antibiotics (2018) 71:826–830
https://doi.org/10.1038/s41429-018-0073-8

JARA Japan Antibiotics Research Association
The Society for Actinomycetes Japan

BRIEF COMMUNICATION

Macrolide and phenolic metabolites from the marine-derived fungus *Paraconiothyrium* sp. VK-13 with anti-inflammatory activity

Tran Hong Quang[1] · Dong Cheol Kim[2,3] · Phan Van Kiem[1] · Chau Van Minh[1] · Nguyen Xuan Nhiem[1] · Bui Huu Tai[1] · Pham Hai Yen[1] · Nguyen Thi Thanh Ngan[4] · Hye Jin Kim[2] · Hyuncheol Oh[2,3]

Received: 2 February 2018 / Revised: 15 May 2018 / Accepted: 22 May 2018 / Published online: 26 June 2018

Abstract

Five new secondary metabolites, modiolides D-G (**1**−**4**) and 1-(2,5-dihydroxyphenyl)-3-methoxy-butan-1-one (**8**), one new natural product, 1-(2,5-dihydroxyphenyl)-3-hydroxybutan-1-one (**7**), along with three known compounds, modiolides A (**5**) and B (**6**), and 1-(2,5-dihydroxyphenyl)-2-buten-1-one (**9**) were isolated from a fermentation culture of the marine endophytic fungus *Paraconiothyrium* sp. VK-13. Their chemical structures were elucidated by the NMR and MS spectroscopic analysis as well as the modified Mosher's method. Compounds **7** and **9** inhibited the overproduction of proinflammatory mediators NO and PGE_2 in LPS-stimulated RAW264.7 cells, with IC_{50} values ranging from 3.9 to 12.5 μM. The inhibitory effects of **7** and **9** on the release of NO and PGE_2 were correlated with their significant suppression of iNOS and COX-2 protein expression, respectively. Furthermore, both compounds **7** and **9** inhibited the mRNA expression of proinflammatory cytokines, including TNF-α, IL-1β, IL-6, and IL-12, with IC_{50} values in a range of 2.4−12.5 μM.

The fungi of the genus *Paraconiothyrium* have been shown to produce different classes of secondary metabolites, including sesquiterpenoids, diterpenoids, isoprenoid decalins, furanones, polyketides, and dihydrocoumarins, of which some compounds displayed cytotoxic and antibacterial activities. In the present study, we report the isolation and structural elucidation of five new secondary metabolites and three known compounds, modiolides A (**5**) and B (**6**) [1] and 1-(2,5-dihydroxyphenyl)-2-buten-1-one (**9**) [2] (Fig. 1a) from the EtOAc extract of the fungal strain *Paraconiothyrium* sp. VK-13 along with their in vitro anti-inflammatory activity.

The molecular formula of **1** was established as $C_{12}H_{16}O_5$ by a sodium adduct ion $[M+Na]^+$ at *m/z* 263.0890 in the HRESIMS. The ^1H NMR spectrum of **1** contained signals for one *cis*- and one *trans*-configured double bond, two oxymethine protons, and two methyl groups. The ^{13}C NMR and DEPT spectra showed 12 carbon signals, including two carbonyl carbons at δ_C 169.8 and 171.6, four sp^2 methine carbons, three sp^3 oxygenated methines, one sp^3 methylene, and two methyl carbons (Table 1). Based on these observations, compound **1** was suggested to possess the ten-membered macrolide skeleton [1]. By HSQC and COSY analysis, the spin system ranging from H-2 to H_3-10 was established (Fig. 1b). Comparison of the ^{13}C NMR data of **1** with those of the reported ten-membered macrolide derivative, modiolide A revealed that the structures of both compounds are nearly identical, except for the additional presence of an acetyl group in **1** [1]. The location of the acetyl group at C-4 was established by an HMBC correlation from 5.81 (H-4) to 171.6 (Fig. 1b). In the NOESY spectrum, H-9 showed NOE correlation with H-7,

Electronic supplementary material The online version of this article (https://doi.org/10.1038/s41429-018-0073-8) contains supplementary material, which is available to authorized users.

✉ Phan Van Kiem
phankiem@yahoo.com

✉ Hyuncheol Oh
hoh@wku.ac.kr

[1] Institute of Marine Biochemistry, Vietnam Academy of Science and Technology (VAST), 18 Hoang Quoc Viet, Cau Giay, Hanoi, Vietnam

[2] College of Pharmacy, Wonkwang University, Iksan 54538, Republic of Korea

[3] Hanbang Cardio-Renal Syndrome Research Center, Wonkwang University, Iksan 54538, Republic of Korea

[4] Institute of Genome Research, Vietnam Academy of Science and Technology (VAST), 18 Hoang Quoc Viet, Cau Giay, Hanoi, Vietnam

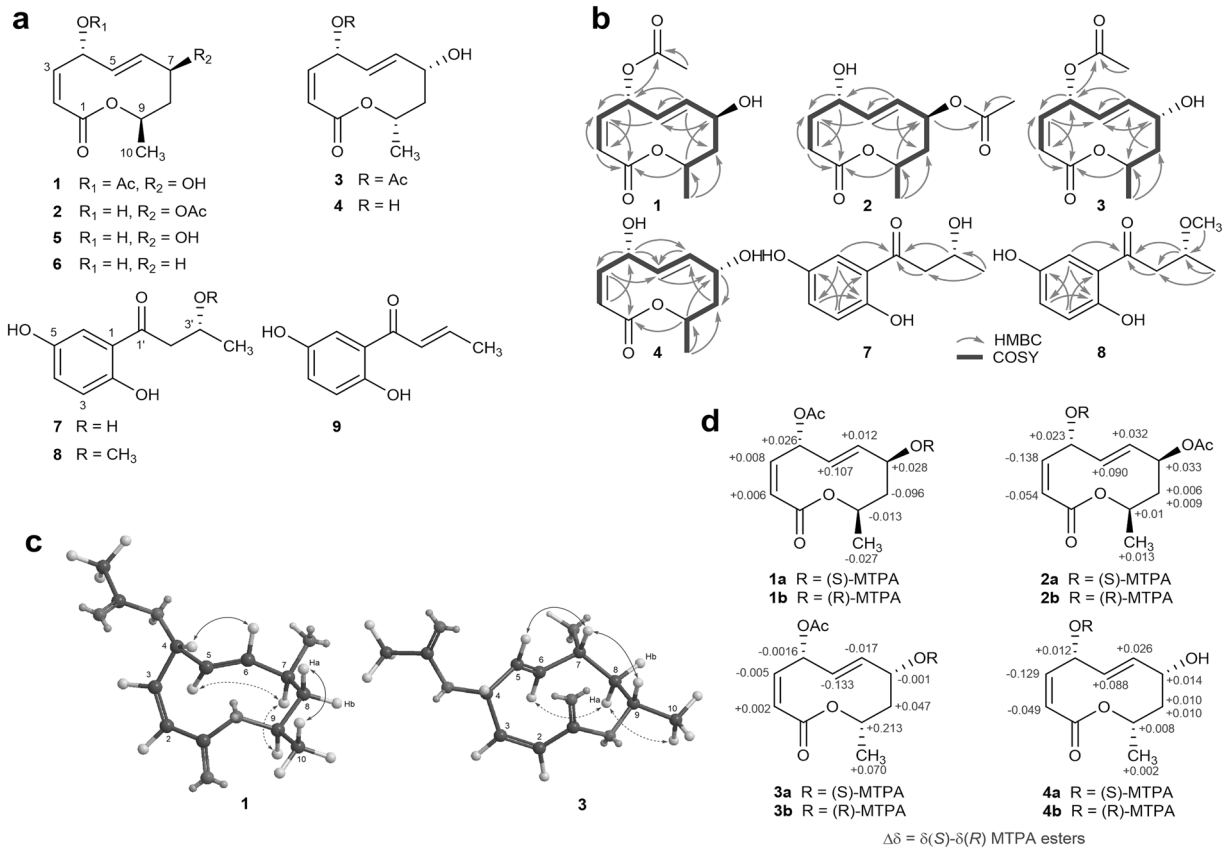

Fig. 1 **a** Chemical structures of compounds **1**–**9**; **b** the selected HMBC and COSY correlations of compounds **1**–**4, 7**, and **8**; **c** the selected NOESY correlations of compounds **1** and **3**; **d** ^{1}H NMR chemical shift differences of MTPA esters of compounds **1**–**4**

suggesting that H-7 and H-9 have the same orientation (Fig. 1c). The opposite orientations of Ha-8 and H_3-10 were deduced by NOE cross-peaks between these protons. Furthermore, H-7 showed an NOE correlation with H-5, while H-6 correlated with H-4, revealing that H-4 and H-7 have opposite orientations. NOE correlations of **1** were found to be in a good agreement with those of the reported analog, modiolide A, suggesting that both compounds have the same relative configuration [1]. Finally, the absolute configuration of **1** was determined using the modified Mosher's method [3]. Calculation of Δδ values for protons neighboring C-7 led to identification of 7*S* configuration (Fig. 1d). Thus, the gross structure of **1** was established as (2*Z*,4*R*,5*E*,7*S*,9*R*)-4-*O*-acetyl-7-hydroxy-9-methyl-2,5-nonadien-9-olide, named modiolide D.

The molecular formula of **2**, $C_{12}H_{16}O_5$ was deduced by the HRESIMS: *m/z* 263.0892 $[M+Na]^+$. Comparative analysis of the ^{1}H and ^{13}C NMR data of **2** with those of **1** suggested that the structures of these compounds are nearly identical, except for the different location of the acetyl functional group (Table 1). The location of the acetyl group at C-7 was deduced by an HMBC correlation from δ_H 5.22 (H-7) to δ_C 171.6 (Fig. 1b). NOESY correlations of **2** were shown to be similar with those of **1**, suggesting that both compounds have the same relative configuration. The absolute configuration of C-4 was identified as *R* (Fig. 1d) by the modified Mosher's method. Therefore, the structure of **2** was established as (2*Z*,4*R*,5*E*,7*S*,9*R*)-4-hydroxy-7-*O*-acetyl-9-methyl-2,5-nonadien-9-olide, named modiolide E.

The HRESIMS of **3** showed an ion peak $[M+Na]^+$ at *m/z* 263.0893, corresponding with the molecular formula $C_{12}H_{16}O_5Na$. Comparison of the ^{13}C NMR values of **3** with those of **1** showed that the chemical shifts of the C-7, C-8, and C-9 of **3** are shifted to further upfield regions, suggesting that these compounds have different configurations at C-7 and C-9 positions (Table 1). Indeed, the absolute configuration of C-7 was determined to be *R* by the modified Mosher's method (Fig. 1d). In the NOESY spectrum, NOE correlations of H-7 with H-5 and H-9 revealed that these protons are oriented to the β-face of the molecule (Fig. 1c). NOE correlations between H-6 and Ha-8 and between Ha-8 and H_3-10 indicated that Ha-8 and H_3-10 are both α-oriented. Thus, the structure of **3** was identified as (2*Z*,4*R*,5*E*,7*R*,9*S*)-4-*O*-acetyl-7-hydroxy-9-methyl-2,5-nonadien-9-olide, named modiolide F.

Compound **4** has the molecular formula $C_{10}H_{14}O_4$ as deduced by the HRESIMS: *m/z* 221.0772 $[M+Na]^+$. The ^{1}H and ^{13}C NMR spectroscopic data revealed that **4** is a

Table 1 ^{1}H and ^{13}C NMR data for compounds **1**–**4**

No	**1**		**2**		**3**		**4**	
	δ_C[a,b]	δ_H[a,c] (*J* in Hz)	δ_C[a,b]	δ_H[a,c] (*J* in Hz)	δ_C[a,b]	δ_H[a,c] (*J* in Hz)	δ_C[a,b]	δ_H[a,c] (*J* in Hz)
1	169.8		169.9		169.8		170.3	
2	125.6	6.03 (dd, 1.6, 12.4)	122.9	5.90 (dd, 1.6, 12.8)	125.5	5.98 (dd, 2.0, 12.4)	122.8	5.83 (br d, 12.4)
3	133.3	5.79 (dd, 3.6, 12.4)	137.8	5.84 (dd, 3.6, 12.8)	133.6	5.78 (dd, 3.2, 12.4)	138.2	5.82 (dd, 3.6, 12.4)
4	73.9	5.81 (ddd, 1.6, 3.2, 8.0)	71.9	4.69 (br d, 8.0)	74.7	5.86 (br d, 7.6)	72.8	4.73 (br d, 6.8)
5	126.6	5.60 (dd, 8.4, 16.0)	134.0	5.77 (dd, 8.4, 16.0)	121.7	5.71 (ddd, 2.0, 8.0, 16.0)	125.9	5.75 (ddd, 2.0, 6.4, 16.0)
6	140.9	5.71 (dd, 8.8, 16.0)	133.9	5.60 (dd, 9.2, 16.0)	140.6	5.95 (dd, 2.4, 16.0)	138.3	5.76 (ddd, 0.8, 1.6, 16.0)
7	72.7	4.12 (m)	75.2	5.22 (m)	67.9	4.49 (m)	67.9	4.48 (br)
8	43.8	1.90 (ddd, 2.0, 3.2, 14.0) 1.74 (dt, 3.2, 14.0)	40.7	1.95 (ddd, 1.6, 2.8, 13.6) 1.85 (dt, 2.8, 13.6)	41.2	1.85 (m) 1.82 (m)	41.3	1.83 (m) 1.81 (m)
9	70.3	5.26 (m)	69.8	5.30 (m)	67.7	5.56 (m)	67.6	5.54 (m)
10	21.5	1.24 (d, 6.4)	21.5	1.24 (d, 6.4)	21.4	1.19 (d, 6.4)	21.5	1.18 (d, 6.4)
Ac	171.6 20.9	2.04 (s)	171.6 21.1	1.99 (s)	171.8 20.9	2.03 (s)		

[a]Recorded in CD_3OD

[b]100 MHz

[c]400 MHz

Table 2 ^{1}H and ^{13}C NMR data for compounds **7** and **8**

Position	**7**		**8**	
	δ_C[a,b]	δ_H[a,c] (*J* in Hz)	δ_C[a,b]	δ_H[a,c] (*J* in Hz)
1	120.7		120.9	
2	150.4		150.6	
3	119.6	6.77 (d, 8.8)	119.7	6.79 (d, 8.8)
4	125.9	6.98 (dd, 2.8, 8.8)	125.9	7.00 (dd, 2.8, 8.8)
5	156.6		156.7	
6	115.9	7.20 (d, 2.8)	115.9	7.23 (d, 2.8)
1′	206.2		205.9	
2′	48.3	3.15 (dd, 7.6, 16.4) 3.00 (dd, 4.8, 16.4)	46.3	3.27 (dd, 7.2, 16.0) 2.95 (dd, 5.6, 16.0)
3′	65.2	4.36 (m)	74.9	3.97 (q, 6.4)
4′	23.5	1.26 (d, 6.4)	19.7	1.25 (d, 6.0)
3′-OCH_3			56.7	3.32 (s)

[a]Recorded in CD_3OD

[b]100 MHz

[c]400 MHz

ten-membered macrolide. Comparison of the ^{1}H and ^{13}C NMR data of **4** with those of the reported ten-membered macrolide, modiolide A resulted in the close similarity, except that the chemical shifts of C-7, C-8, and C-9 in **4** are more upfield shifted [1], suggesting that these compounds are diastereomers at the C-7 and C-9 positions. This suggestion was supported by comparing the carbon chemical shifts of C-7, C-8, and C-9 between **4** and **3** (Table 1). The relative configuration of **4** was shown to be the same as that of **3**, as deduced by NOESY spectroscopic analysis. In addition, considering the chemical shift differences observed between **4** and modiolide A, the overall structure of **4** was suggested to be a diasteromer of modiolide A, having inverted configuration at C-7 and C-9 because the absolute configuration of C-4 was determined to be *R* by application of the modified Mosher's method (Fig. 1d). Although the stereochemistry of **4** was shown to be similar with that of the previously reported macrolide, fusanolide B [4], the proton and carbon chemical shifts of C-7, C-8, and C-9 of these compounds were significantly different [**4** (in CD_3OD): δ_H 4.48 (H-7)/ δ_C 67.9 (C-7), δ_H 1.83 and 1.81 (H_2-8)/ δ_C 41.3 (C-8), δ_H 5.54 (H-9)/ δ_C 67.6 (C-9) vs. fusanolide B (in CD_3OD): δ_H 4.12 (H-7)/ δ_C 73.7 (C-7), δ_H 1.90 and 1.73 (H_2-8)/ δ_C 44.8 (C-8), δ_H 5.25 (H-9)/ δ_C 71.0 (C-9)]. Furthermore, the ^{1}H and ^{13}C NMR data of the reported fusanolide B were identical with those of modiolide A, revealing that both compounds have the same configuration [1, 4]. This evidence allowed to revise the configuration of fusanolide B to be the same as that of modiolide A and conclude that **4** is a diastereomer of both fusanolide B and modiolide A. Thus, the structure of **4** was determined to be (2*Z*,4*R*,5*E*,7*R*,9*S*)-4,7-dihydroxy-9-methyl-2,5-nonadien-9-olide, named modiolide G.

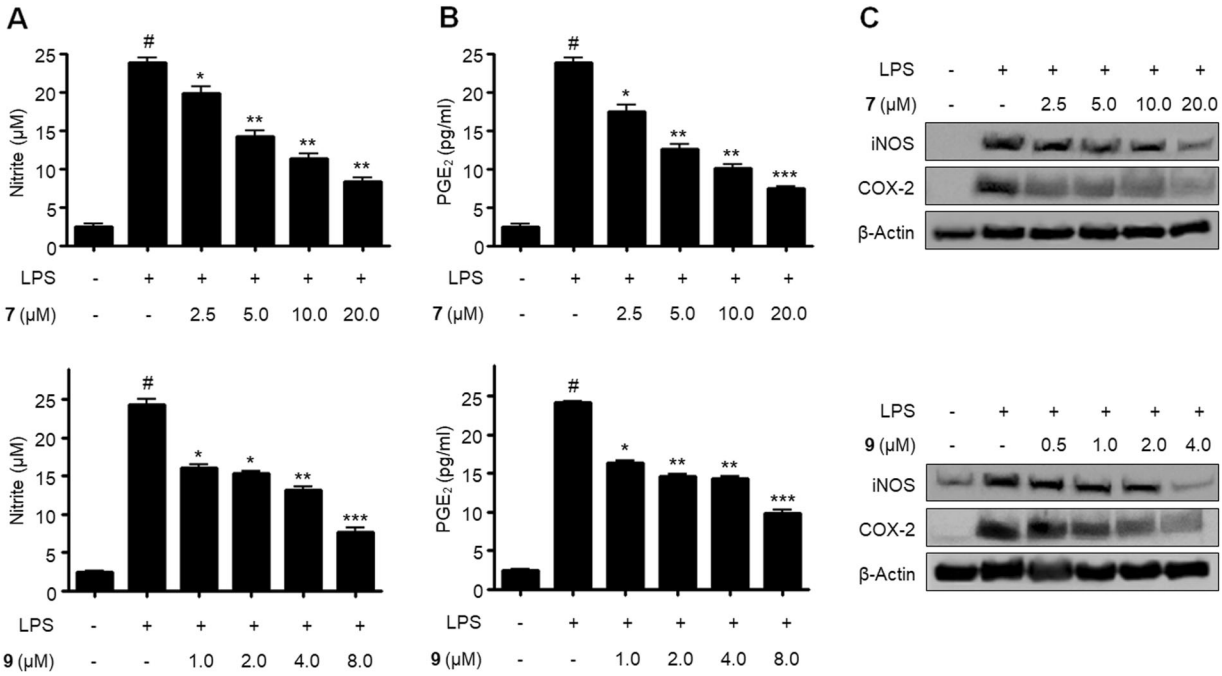

Fig. 2 Effects of compounds **7** and **9** on nitrite (**a**) and PGE_2 (**b**) production and iNOS and COX-2 protein expression (**c**) in LPS-stimulated RAW264.7 macrophages. Data represent the mean values of three experiments (±SD). $^{\#}p < 0.01$ versus control groups; $^{*}p < 0.05$ and $^{**}p < 0.01$ compared to the group treated with LPS only

Analysis of the NMR and HRESIMS (*m/z* 219.0633 $[M+Na]^+$) data of **7** suggested that **7** is a phenyl-1-butanone derivative [5]. Assignment of all positions of the structure of **7** was done by comparison of the ^1H and ^{13}C NMR data of **7** with those of the reported analogs [5–8], as well as analysis of HSQC and HMBC spectra (Fig. 1b). The stereochemistry of C-3′ was proposed to be *R* by comparing the proton and carbon chemical shifts of C-3′ and the specific optical rotation of **7** with those of the reported compounds [8]. Thus, the structure of **7** was established as 1-(2,5-dihydroxyphenyl)-3-hydroxybutan-1-one.

Compound **8** possesses the molecular formula $C_{11}H_{14}O_4$ as determined by the HRESIMS: *m/z* 233.0794 $[M+Na]^+$. The ^1H and ^{13}C NMR data of **8** were found to be almost identical with those of **7**, except for the addition of a methoxy group [δ_H 3.32 (s)/δ_C 56.7] in **8** (Table 2). The location of the methoxy group at C-3′ was deduced by an HMBC correlation observed from δ_H 3.32 to δ_C 74.9 (C-3′) in the HMBC spectrum (Fig. 1b). Therefore, the structure of **8** was identified as 1-(2,5-dihydroxyphenyl)-3-methoxybutan-1-one. The absolute configuration **8** was proposed to be analogous to that of **7**.

Excessive production of NO during acute and chronic inflammation is associated with the development of many inflammatory disorders and cancer [9–12]. Therefore, we initially evaluated the inhibitory effects of the isolated compounds on the NO overproduction in LPS-stimulated RAW264.7 cells at 20 μM [13]. The result showed that only **7** and **9** inhibit the nitrite production among the compounds tested (data not shown). Based on the screening data, **7** and **9** were chosen to examine their effects on overproduction of nitrite and PGE_2 in LPS-stimulated RAW264.7 cells at different concentrations [14]. Firstly, to exclude the possibility of cytotoxicity, the viability of RAW264.7 cells was evaluated in the presence of **7** and **9** by MTT assay [15]. The result revealed that **7** and **9** are both nontoxic towards RAW264.7 cells at 20 μM. The cells were then pretreated for 12 h with different concentrations of **7** and **9**, followed by treatment with LPS (1 μg/mL) for 18 h (see Supplementary information). Figure 2a showed that nitrite concentration in only LPS-treated group is increased nine-fold compared with that of the untreated group. However, pretreatment of the cells with **7** and **9** decreased nitrite production in a dose-dependent manner (Fig. 2a), with IC_{50} values of 12.5 and 3.9 μM, respectively (Table S1). Similarly, the production of PGE_2 in LPS-stimulated RAW264.7 cells was suppressed by **7** and **9** (Fig. 2b), with IC_{50} values of 9.5 and 6.9 μM, respectively (Table S1).

During the inflammatory process, the proinflammatory mediators NO and PGE_2 are released by the activities of their inducible enzymes, iNOS and COX-2, respectively [16, 17]. Accordingly, downregulation of iNOS and COX-2 protein expression decreases the secretion of the proinflammatory and cytotoxic mediators [14, 18]. Thus, we next examined the effects of **7** and **9** on iNOS and COX-2 protein expression in LPS-stimulated RAW264.7 cells using western blot analysis. When treating with LPS, the expression of iNOS and COX-2 protein levels in the cells were shown to be remarkably

upregulated compared with the untreated groups (Fig. 2c). However, **7** and **9** both attenuated LPS-induced iNOS and COX-2 expression in a dose-dependent manner, suggesting that **7** and **9** inhibit the NO and PGE_2 production through downregulation of iNOS and COX-2 protein expression, respectively. Next, we investigated the effects of **7** and **9** on TNF-α, IL-1β, IL-6, and IL-12 mRNA expression in LPS-stimulated RAW264.7 macrophages using quantitative real-time reverse transcriptase-polymerase chain reaction (qRT-PCR). As the result, **9** inhibited TNF-α, IL-1β, IL-6, and IL-12 mRNA expression, with IC_{50} values of 4.2, 2.4, 2.6, and 3.3 μM, respectively; while **7** attenuated TNF-α, IL-1β, IL-6, and IL-12 mRNA expression, with IC_{50} values of 12.5, 11.7, 10.6, and 13.5 μM, respectively (Table S1). These results revealed that both **7** and **9** inhibit the proinflammatory cytokine gene expression at the transcriptional level.

Acknowledgements This work was financially supported by Vietnam Academy of Science and Technology (VAST.HTQT.HANQUOC.03/17-18) and the framework of international cooperation program managed by the National Research Foundation of Korea (2016K2A9A1A06924074, FY2016). Additional research support was provided through the National Research Foundation of Korea (NRF) grants funded by the Korea government (NRF-2017R1A5A2015805).

Compliance with ethical standards

Conflict of interest The authors declare that they have no conflict of interest.

References

1. Tsuda M, et al. Modiolides A and B, two new 10-membered macrolides from a marine-derived fungus. J Nat Prod. 2003;66:412–5.
2. Kraus GA, Kirihara M. Quinone photochemistry. A general synthesis of acylhydroquinones. J Org Chem. 1992;57:3256–7.
3. Ohtani I, Kusumi T, Kashman Y, Kakisawa H. High-field FT NMR application of Mosher's method. The absolute configurations of marine terpenoids. J Am Chem Soc. 1991;113:4092–6.
4. Shimada A, et al. Pollen growth regulator, fusanolide A, and a related metabolite from *Fusarium* sp. Z Naturforsch B Chem Sci. 2002;57:239–42.
5. Musa MM, Ziegelmann-Fjeld KI, Vieille C, Zeikus JG, Phillips RS. Asymmetric reduction and oxidation of aromatic ketones and alcohols using W110A secondary alcohol dehydrogenase from *Thermoanaerobacter ethanolicus*. J Org Chem. 2007;72:30–34.
6. Yang KS, Nibbs AE, Turkmen YE, Rawal VH. Squaramide-catalyzed enantioselective Michael addition of masked acyl cyanides to substituted enones. J Am Chem Soc. 2013;135:16050–3.
7. Liu Z, et al. Preparative isolation and purification of acetophenones from the Chinese medicinal plant *Cynanchum bungei* Decne. by high-speed counter-current chromatography. Sep Purif Technol. 2008;64:247–52.
8. Ahmad K, et al. Enzyme directed diastereoselectivity in chemical reductions: studies towards the preparation of all four isomers of 1-phenyl-1,3-butanediol. Tetrahedron: Asymmetry. 2004;15:1685–92.
9. Sharma JN, Al-Omran A, Parvathy SS. Role of nitric oxide in inflammatory diseases. Inflammopharmacology. 2007;15:252–9.
10. Dawson VL, Dawson TM. Nitric oxide in neurodegeneration. Prog Brain Res. 1998;118:215–29.
11. Liew FY. Regulation of nitric oxide synthesis in infectious and autoimmune diseases. Immunol Lett. 1994;43:95–98.
12. Maeda H, Akaike T. Nitric oxide and oxygen radicals in infection, inflammation, and cancer. Biochem (Mosc). 1998;63:854–65.
13. Titheradge MA. The enzymatic measurement of nitrate and nitrite. Methods Mol Biol. 1998;100:83–91.
14. Ngan NT, et al. Anti-inflammatory effects of secondary metabolites isolated from the marine-derived fungal strain *Penicillium* sp. SF-5629. Arch Pharm Res. 2017;40:328–37.
15. Mosmann T. Rapid colorimetric assay for cellular growth and survival: application to proliferation and cytotoxicity assays. J Immunol Methods. 1983;65:55–63.
16. Guzik TJ, Korbut R, Adamek-Guzik T. Nitric oxide and superoxide in inflammation and immune regulation. J Physiol Pharmacol. 2003;54:469–87.
17. Tzeng SF, Hsiao HY, Mak OT. Prostaglandins and cyclooxygenases in glial cells during brain inflammation. Curr Drug Targets Inflamm Allergy. 2005;4:335–40.
18. Kim DC, et al. Dihydroisocoumarin derivatives from marine-derived fungal isolates and their anti-inflammatory effects in lipopolysaccharide-induced BV2 microglia. J Nat Prod. 2015;78:2948–55.